

## Motivation

The objective of this work is to show the interest of GNSS for weather forecasts, especially for nowcasting. We will focus on GPS observations (post-processing with a time resolution of 15 minutes) and try to answer the following question:

*"Can the detection of integrated water vapour (IWP) by GNSS allow us to establish typical configurations of humidity field which characterize convective systems and particularly which supply forerunners of their initialization associated to a deep convection?"*

To validate our typical water vapour configurations by GNSS, called **H<sub>2</sub>O alert**, we will use detection of precipitation by C-band weather radar and thermal infrared radiance of the 10.8- $\mu$ m channel (Ch09) of SEVIRI instrument on METEOSAT Second Generation.

## Case study: 28-29<sup>th</sup> June 2005 rainfall event

Between 10:00 am and 4:00 pm UTC, surface analyses indicate a convective episode over Belgium. Using Belgian synoptic network lines of convergences have been identified. These are associated with a low barometric hollow as shown at 12H UTC (2010/06/29) Figure 1.

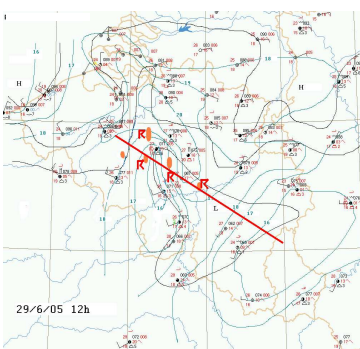
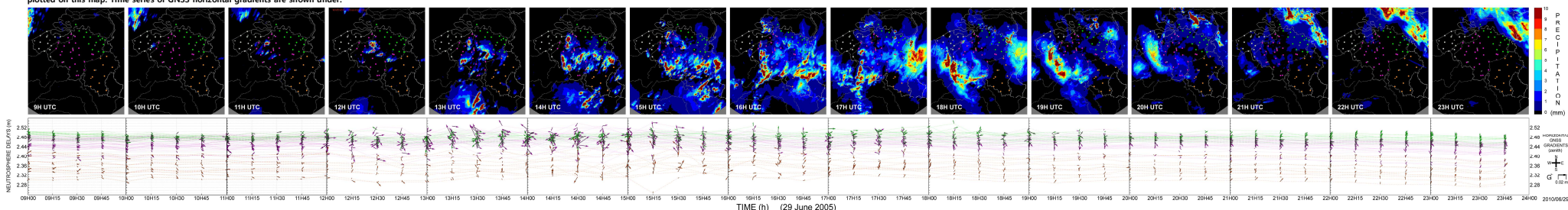


Figure 1: Meso-scale surface analysis. Plot of a line of convergence is shown in red, radar precipitation in orange, and R symbol for thunderstorms detected by SAFIR.

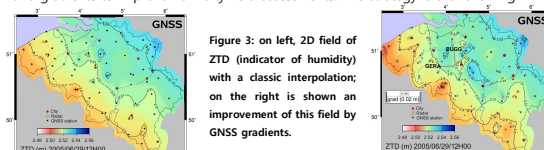
Using the synoptic network and near-real time meteorological observations (radar, SAFIR, METEOSAT), forecast of rainfalls induced by the several convective systems was not possible for such a tricky situation.

Figure 2: Sequence of hourly precipitations detected by radar from 9H to midnight (29 June 2005). GNSS stations are plotted on this map. Time series of GNSS horizontal gradients are shown under.



## Improvement of humidity field by GNSS gradients

Since 1992 [Bevis et al.] GNSS allows us an estimation of the humidity field. We have measured ZTD and horizontal gradients of delay [Chen and Herring, 1997] with GAMIT. Using the Belgian Dense Network (baseline from 5 to 30 km) we have combined ZTD and gradients to improve humidity field assessments. The strategy is the following:



In the direction shown by gradient two additional ZTD pseudo-observations (more wet and drier) have been considered. Our tests have shown that 10 km on either side of the GNSS site is the most relevant distance for our network to detect small scale structures of the troposphere as convective systems. We have used Walpersdorf et al. [2001] to estimate additional ZTDs with altitude correction [Vedel et al., 2001]. The module of the horizontal gradient (at 10°) is mapped in the zenith direction with Niell Mapping Function [Niell, 1996].

The meteorological situation and the location of water vapour bubbles observed by GNSS show a good agreement with radar precipitation. We can see figure 2 that tropospheric activity is detected by GNSS gradients. The next step has been to implement H<sub>2</sub>O alert according to a specific configuration of GNSS humidity field.

## Indicators of deep convection

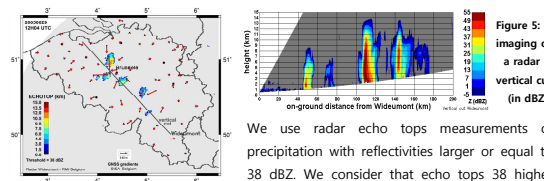


Figure 4: echo top radar (38 dBZ). Black line show the location of the vertical cut of radar reflectivity (Fig. 5). GNSS gradients are plotted.

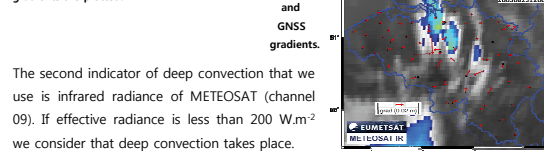


Figure 5: imaging of a radar vertical cut (in dBZ).

We use radar echo tops measurements of precipitation with reflectivities larger or equal to 38 dBZ. We consider that echo tops 38 higher than 5 km are an indicator of deep convection.

Figure 6: infrared radiance of the 10.8- $\mu$ m channel of SEVIRI and GNSS gradients.

Figure 6: infrared radiance of the 10.8- $\mu$ m channel of SEVIRI and GNSS gradients.

The second indicator of deep convection that we use is infrared radiance of METEOSAT (channel 09). If effective radiance is less than 200 W.m<sup>-2</sup> we consider that deep convection takes place.

## Implementation H<sub>2</sub>O alert by GNSS

A meticulous observation of ZTD and gradients time-series have shown that a typical configuration can be observed before initiation of deep convection (see Fig.7). Using improvement of humidity field by gradients we have established gridded map of GNSS alert with a high resolution (3 km X 3.5 km).

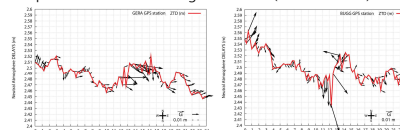


Figure 7: time-series of ZTD and gradients for GERA and BUGG stations (29 June 2005).

The conditions to obtain **H<sub>2</sub>O alert** at the time T are the following:

ZTD decrease of 0.008 m from T-30 min to T-15 min

ZTD increase of 0.015 m from T-15 min to T

## First results of H<sub>2</sub>O alert validation

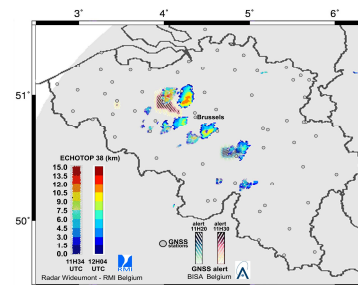


Figure 8: GNSS H<sub>2</sub>O alert and radar echo tops 38 (2005/06/29).

To estimate the score of our H<sub>2</sub>O alert by GNSS we consider that an alert is validated if an indicator of deep convection (by radar and/or by SEVIRI) takes place 45 minutes after this alert. Alert and indicator are established for the same grid (pixel 3 km X 3.5 km).

Periods	Number of H <sub>2</sub> O alerts	Score (radar)	Score (SEVIRI)	Final Score
2005/06/27	0	0	0	0
2005/06/28	1853	31%	71%	75%
2005/06/29	6384	44%	84%	87%
2005/06/30	0	0	0	0
All days	8237	41%	81%	84%

Table 1: first statistics results. For each H<sub>2</sub>O alert (pixel), if deep convection is indicated by radar and/or SEVIRI, one count is obtained. Final scores are set with a normalization in percentage.

## Conclusion and perspective

This study has shown that our GNSS H<sub>2</sub>O alerts which take into account a dry-wet contrast of the humidity are a good indicator of deep convection (validation by radar and SEVIRI). We have shown the key role of GNSS horizontal gradient to detect water vapour bubbles and associated contrasts of humidity which are forerunners of deep convection.

Nevertheless we need to validate our alert with NRT ZTD measurements. In addition, an absolute precondition to increase the scores of these alerts and to use them operationally for nowcasting is to combine them with NWP. Then a precise location of the convective system could be obtained.

## References

- Bevis, M., S. Businger, T. A. Herring, C. Rocken, R. A. Anthes, and R. H. Ware, GPS meteorology: Remote sensing of atmospheric water vapor using the Global Positioning System, J. Geophys. Res., 97(D14), 15,787-15,801, 1992.
- Chen, G. and T. A. Herring, Effects of atmospheric azimuthal asymmetry on the analysis of space geodetic data, J. Geophys. Res., 102, 20,489-20,502, 1997.
- Niell, A.E., Global mapping functions for the atmosphere delay at radio wavelengths, JGR, Vol. 101, No. B2, 3227-3246, 1996.
- Vedel, H., K.S. Mogensen and X.-Y. Huang, Calculation of zenith delays from meteorological data, comparison of NWP model, radiosonde and GPS delays. Physics and Chemistry of the Earth, 26A, pp 497-502, 2001.
- Walpersdorf, A., E. Calais, J. Haase, L. Eymard, M. Desbois and H. Vedel, Atmospheric gradients estimated by GPS compared to a high resolution numerical weather prediction (NWP) model. Physics and Chemistry of the Earth, Part A: Solid Earth and Geodesy, Vol. 26 (3) pp. 147-152, 2001.